Journal of Biological Dynamics
Publication details, including instructions for authors and subscription information:
http://www.tandfonline.com/loi/tjbd20

On the global stability of a generalized cholera epidemiological model

Yuanji Cheng [a], Jin Wang [b] & Xiuxiang Yang [c]

[a] School of Technology, Malmö University, 205 06, Malmö, Sweden E-mail:

[b] Department of Mathematics and Statistics, Old Dominion University, Norfolk, VA, 23529, USA

[c] Department of Mathematics, Weinan Normal University, Weinan 714000, Shaanxi, People's Republic of China E-mail:

Version of record first published: 30 Oct 2012.

To cite this article: Yuanji Cheng, Jin Wang & Xiuxiang Yang (2012): On the global stability of a generalized cholera epidemiological model, Journal of Biological Dynamics, 6:2, 1088-1104

To link to this article: http://dx.doi.org/10.1080/17513758.2012.728635

Journal of Biological Dynamics
Vol. 6, No. 2, March 2012, 1088–1104

Taylor & Francis
Taylor & Francis Group

On the global stability of a generalized cholera epidemiological model

Yuanji Cheng[a], Jin Wang[b]* and Xiuxiang Yang[c]

[a]*School of Technology, Malmö University, 205 06 Malmö, Sweden;* [b]*Department of Mathematics and Statistics, Old Dominion University, Norfolk, VA 23529, USA;* [c]*Department of Mathematics, Weinan Normal University, Weinan 714000, Shaanxi, People's Republic of China*

(*Received 16 January 2012; final version received 31 August 2012*)

In this paper, we conduct a careful global stability analysis for a generalized cholera epidemiological model originally proposed in [J. Wang and S. Liao, *A generalized cholera model and epidemic/endemic analysis*, J. Biol. Dyn. 6 (2012), pp. 568–589]. Cholera is a water- and food-borne infectious disease whose dynamics are complicated by the multiple interactions between the human host, the pathogen, and the environment. Using the geometric approach, we rigorously prove the endemic global stability for the cholera model in three-dimensional (when the pathogen component is a scalar) and four-dimensional (when the pathogen component is a vector) systems. This work unifies the study of global dynamics for several existing deterministic cholera models. The analytical predictions are verified by numerical simulation results.

Keywords: cholera modelling; global asymptotic stability; geometric approach

1. Introduction

Cholera, a severe water- and food-borne infectious disease caused by the gram negative bacterium *Vibrio cholerae*, remains a significant public health burden in the developing world, despite a large body of clinical and theoretical studies [1,10,12,20,33,36–38,45] and tremendous efforts in prevention and intervention [48]. This is partly due to the limited understanding at present on the complex infection dynamics of cholera, which involve both direct human-to-human and indirect environment-to-human transmission pathways.

Over the last decade, quite a few mathematical models have been published to investigate the transmission dynamics of cholera. For example, Codeço in 2001 proposed a model [5] that explicitly accounted for the environmental component, i.e. the *V. cholerae* concentration in the water supply, into a regular SIR epidemiological model. The incidence (or the infection force) was modelled by a saturating function $aS(B/(K+B))$ to represent the effect of saturation, where S is the

*Corresponding author. j3wang@odu.edu
Author Emails: yuanji.cheng@mah.se; yangxiuxiang2000@yahoo.com.cn
This paper is based on an invited talk given at the 3rd International Conference on Math Modeling & Analysis, San Antonio, USA, October 2011.

ISSN 1751-3758 print/ISSN 1751-3766 online

http://dx.doi.org/10.1080/17513758.2012.728635
http://www.tandfonline.com

susceptible population, B is the pathogen concentration, a is the contact rate with contaminated water, and K is the half saturation rate (i.e. the infectious dose in water sufficient to produce disease in 50% of those exposed). Hartley *et al.* [13] in 2006 extended Codeço's work to include a hyperinfectious (HI) state of the pathogen, representing the 'explosive' infectivity of freshly shed *V. cholerae*, based on the laboratory observations [1,33]. They modelled the incidence factor by $\beta_{\mathrm{L}}S(B_{\mathrm{L}}/(\kappa_{\mathrm{L}}+B_{\mathrm{L}}))+\beta_{\mathrm{H}}S(B_{\mathrm{H}}/(\kappa_{\mathrm{H}}+B_{\mathrm{H}}))$ where β_{H} and β_L are the HI and less-infectious (LI) ingestion rates, and κ_{H} and κ_L are the HI and LI half saturation rates. This model was rigorously analysed in [30]. Joh *et al.* [18] in 2009 modified Codeço's model by a threshold pathogen density for infection, with a careful discussion on human–environment contact and in-reservoir pathogen dynamics. More recently, Mukandavire *et al.* [34] proposed a model to study the 2008–2009 cholera outbreak in Zimbabwe. The model explicitly considered both human-to-human and environment-to-human transmission pathways. The incidence was represented by $\beta_{\mathrm{e}}S(B/(K+B))+\beta_{\mathrm{h}}SI$ with I denoting the infected population and β_{e} and β_{h} being the rates of vibrio ingestion from the environment and the human–human interaction, respectively. The results in this work demonstrated the importance of the human-to-human transmission in cholera epidemics, especially in such places as Zimbabwe, a land-locked country in the middle of Africa. Moreover, Tien and Earn [44] in 2010 published a water-borne disease model which also included the dual transmission pathways, with bilinear incidence rates employed for both the environment-to-human and human-to-human infection routes. No saturation effect was considered in Tien and Earn's work.

The afore-mentioned work has certainly made important contribution to the understanding of cholera dynamics. Some limitations of these models, however, are that they only considered bilinear or saturating incidence functions, and they all assumed that the bacterial growth outside of human hosts follows linear dynamics. Practically, the multiple interactions between human population, cholera pathogen, and the environment could be much more complicated. For example, in a cholera model published by Jensen *et al.* [17], the incidence was represented as $\pi(B/(Ck+B))^7S$, a highly nonlinear function, and the growth of *V. cholerae* was also nonlinear (a quadratic function in B). Also, in a recent paper by Shuai and van den Driessche [39], the incidence function is a summation of the form $f_j(S,I_j)+g_j(S,B_j)$ with nonlinear functions f_j and g_j for different infection stages and pathogen concentrations, and the bacterial growth is determined by a nonlinear shedding rate from the infectious human population.

Building on these studies, Wang and Liao [47] in 2011 proposed a generalized cholera epidemiological model which incorporates general incidence and pathogen functions into the multiple transmission pathways, and which unifies many of the existing cholera models. Careful equilibrium analysis has been conducted in [47] and the results are summarized in Theorem 2.2 in Section 2 of the present paper. In particular, the local and global dynamics of the disease-free equilibrium, as well as the existence, uniqueness, and local dynamics of the endemic equilibrium, have been established.

The global stability of the endemic equilibrium for this general model, however, has not been resolved. In fact, to our knowledge, very few studies on cholera modelling have addressed the endemic global dynamics [43]. Thus, some important epidemiological questions, e.g. whether the long-term disease dynamics approaches an equilibrium and how this depends on the initial size of the infection, remain to be answered. The study of the endemic global stability is not only mathematically important, but also essential in predicting the evolution of the disease in the long run so that prevention and intervention strategies can be effectively designed, and public health administrative efforts can be properly scaled. The challenge, however, in the global analysis of cholera models is that due to the incorporation of the environmental components, the models usually constitute high-dimensional nonlinear autonomous systems for which the classical Poincaré–Bendixson theory [14] is no longer valid. The method of monotone flow [23,24,40–42] can be applied to a class of high-dimensional dynamical systems which possesses monotonicity (e.g. competitiveness). Unfortunately, this technique is not applicable to most cholera epidemic

models which are non-monotone. The method based on Lyapunov functions [19,21] is well known for stability analysis, though the fact that there is no systematic way to find Lyapunov functions hinders the application of this approach to many nonlinear systems. Finally, the geometric approach for stability analysis, originally developed by Li and Muldowney [9,25,28], has gained much popularity in recent years, especially in dealing with mathematical epidemic models. Nevertheless, the majority of the applications of the geometric approach is concerned with regular epidemiological models such as SIR, SEIR, SIS, SIRS, or the like. In the present paper, we aim to extend this approach to the endemic global stability analysis of the general cholera model, which is a combined human–environment epidemiological model coupling a SIR model with the pathogen components. Such an extension is nontrivial and, to our knowledge, has not been achieved for epidemiological models of this type before.

We organize the remainder of this paper as follows. In Section 2, we briefly present the generalized cholera model and summarize the results established in [47]. In Section 3, we apply the geometric approach based on the second compound matrix to analyse the three-dimensional system, where the pathogen component is a scalar. In Section 4, we deal with the four-dimensional model where the pathogen component is a vector. The analysis for higher dimensional system is usually more challenging, and the global stability of our four-dimensional system is established by using the geometric approach based on the third compound matrix. In addition, we verify the analytical predictions in Sections 3 and 4 by numerical simulation results. Finally, we close the paper by conclusions in Section 5.

2. Mathematical model

The model consists of the following differential equations:

$$\frac{\mathrm{d}S}{\mathrm{d}t} = bN - Sf(I,B) - bS, \tag{1}$$

$$\frac{\mathrm{d}I}{\mathrm{d}t} = Sf(I,B) - (\gamma + b)I, \tag{2}$$

$$\frac{\mathrm{d}B}{\mathrm{d}t} = h(I,B), \tag{3}$$

together with

$$\frac{\mathrm{d}R}{\mathrm{d}t} = \gamma I - bR. \tag{4}$$

Here S, I , and R denote the susceptible, the infected, and the recovered populations, respectively, and B denotes the concentration of the pathogen in the environment (typically the contaminated water). The total population $N = S + I + R$ is assumed to be a constant. The parameter b represents the natural human birth/death rate, and γ represents the rate of recovery from cholera. The function $f(I,B)$ represents the essential part of the incidence which determines the rate of new infection, whereas the function $h(I,B)$ describes the rate of change for the pathogen in the environment which can be either linear or nonlinear. Both f and h are assumed to be sufficiently smooth to ensure the existence and uniqueness of solutions to the system with non-negative initial conditions. In addition, the component B can be either a scalar or a vector. For example, if we consider both the HI and LI states [13] of the vibrios, then we may write $B = [B_{\mathrm{H}}, B_{\mathrm{L}}]^{\mathrm{T}}$.

Based on biological feasibility, the following conditions for $f(I,B)$ and $h(I,B)$ are assumed for $I \geq 0, B \geq 0$:

(a) $f(0,0) = 0, h(0,0) = 0$;

(b) $f(I,B) \geq 0$;
(c) $\frac{\partial f}{\partial I}(I,B) \geq 0$, $\frac{\partial f}{\partial B}(I,B) \geq 0$, $\frac{\partial h}{\partial I}(I,B) \geq 0$, $\frac{\partial h}{\partial B}(I,B) \leq 0$;
(d) $f(I,B)$ and $h(I,B)$ are concave; i.e. the matrices $D^2 f$ and $D^2 h$ are negative semi-definite.

Here and in what follows, we write a vector $V \geq 0$ (≤ 0) if each component of V is ≥ 0 (≤ 0); we write a matrix $A \geq 0$ (≤ 0) if A is positive (negative) semi-definite.

The article [47] conducted some analysis on this model. Based on the next-generation matrix approach [8], the basic reproduction number R_0 was found by

$$R_0 = \frac{N}{\gamma + b}\left[\frac{\partial f}{\partial I}(0,0) - \frac{\partial f}{\partial B}(0,0)\left(\frac{\partial h}{\partial B}(0,0)\right)^{-1}\frac{\partial h}{\partial I}(0,0)\right]. \tag{5}$$

Remark 2.1 We note that the last inequality in assumption (c) above is based on the experimental observation that the pathogen *V. cholerae* cannot maintain a stable population in the environment in the absence of the inflow from contaminated sewage [5]. This assumption has been used in several existing cholera models (e.g. [5,13,34,44]). In addition, when B is a vector, $\partial h/\partial B$ is a matrix. To ensure that R_0 is positive, we will further assume that $-\partial h/\partial B$ is an M-matrix (i.e. a non-singular square matrix with non-positive off-diagonal entries and all principal minors positive). It is known that the inverse of an M-matrix has all its entries being non-negative [2,7].

Under these assumptions, the equation $h(I,B) = 0$ implicitly defines a function $B = g(I)$ with $g'(I) \geq 0$, and Equation (5) yields

$$R_0 = \frac{N}{\gamma + b}\frac{\partial f}{\partial I}(0,0) + \frac{N}{\gamma + b}\frac{\partial f}{\partial B}(0,0)g'(0) \triangleq R_0^{hh} + R_0^{eh}. \tag{6}$$

Biologically speaking, R_0 measures the average number of secondary infections that occur when one infective is introduced into a completely susceptible host population [8,16,46]. Equation (6) shows that R_0 depends on two factors: one is due to human-to-human transmission (R_0^{hh}) and the other is due to environment-to-human transmission (R_0^{eh}). The term $1/(\gamma + b)$ represents the expected time of the infection, $(\partial f/\partial I)(0,0)$ represents the unit human-to-human transmission rate, and $(N/(\gamma + b))(\partial f/\partial I)(0,0)$ measures the total number of secondary infections caused by the human-to-human transmission. Similarly, the product $(\partial f/\partial B)(0,0)g'(0)$ represents the unit environment-to-human transmission rate, and $(N/(\gamma + b))(\partial f/\partial B)(0,0)g'(0)$ measures the total number of secondary infections caused by the environment-to-human transmission.

It is also shown that there exists a forward transcritical bifurcation at $R_0 = 1$ for this model. Specifically, the following theorem summarizes the dynamics known for the system (1)–(4).

THEOREM 2.2 [47] *When $R_0 < 1$, there is a unique DFE, which is both locally and globally asymptotically stable*; *when $R_0 > 1$, the DFE becomes unstable, and there is a unique positive endemic equilibrium which is locally asymptotically stable.*

3. Three dimensional system

We will now focus our attention on the global asymptotic stability of the endemic equilibrium for $R_0 > 1$. We first consider the case when B is a scalar; i.e. there is only one infectious state (which is assumed to be homogeneous) for the pathogen in the environment. Most cholera models in the literature (e.g. [5,18,34,44]) fall into this category. With the pathogen component being a scalar, the system (1)–(3) is three-dimensional.

The assumption (**d**) implies that the surface $h = h(I, B)$ is below its tangent plane at any point $(I_0, B_0) \geq 0$; that is,

$$h(I, B) \leq h(I_0, B_0) + \frac{\partial h}{\partial I}(I_0, B_0)(I - I_0) + \frac{\partial h}{\partial B}(I_0, B_0)(B - B_0). \tag{7}$$

Particularly, setting $(I_0, B_0) = (0, 0)$ and using the assumption (**a**), we obtain

$$h(I, B) \leq \frac{\partial h}{\partial I}(0, 0)I + \frac{\partial h}{\partial B}(0, 0)B. \tag{8}$$

Thus, Equation (3) yields

$$\frac{\mathrm{d}B}{\mathrm{d}t} \leq \frac{\partial h}{\partial I}(0, 0)I + \frac{\partial h}{\partial B}(0, 0)B \leq \frac{\partial h}{\partial I}(0, 0)N + \frac{\partial h}{\partial B}(0, 0)B, \tag{9}$$

which implies for any initial value $B_0 \leq \omega N$,

$$0 \leq B(t, B_0) \leq \omega N \quad \text{where} \quad \omega = -\frac{(\partial h/\partial I)(0, 0)}{(\partial h/\partial B)(0, 0)}. \tag{10}$$

Therefore, it is clear to see the region

$$\Delta = \{(S, I, B) | S \geq 0, I \geq 0, 0 \leq S + I \leq N, 0 \leq B \leq \omega N\} \tag{11}$$

is a positive invariant domain of the system (1)–(3).

We employ the geometric approach based on the second compound matrix [9,25,28] to analyse the endemic global stability of this system. A brief summary of this technique is provided in Appendix A.

Based on Theorem 2.2, the DFE, $X_0 = (N, 0, 0)$, is unstable when $R_0 > 1$. Since the DFE is on the boundary of the domain Δ, this implies the uniform persistence [11]; i.e. there exists a constant $c > 0$ such that

$$\liminf_{t \to \infty} \{S(t), I(t), B(t)\} > c.$$

Consequently, the uniform persistence and the boundedness of Δ imply that the system has a compact absorbing subset of Δ [4]. Together with Theorem 2.2, we obtain the following result:

PROPOSITION 3.1 *When* $R_0 > 1$, *the system* (1)–(3) *is uniformly persistent*, *and satisfies the assumptions* (H1) *and* (H2) *listed in Appendix A.*

We proceed to verify the Bendixson criterion $\bar{q_2} < 0$ (see Theorem A.1). The Jacobian matrix of the system (1)–(3) is

$$J = \begin{pmatrix} -b - f(I, B) & -S\dfrac{\partial f}{\partial I} & -S\dfrac{\partial f}{\partial B} \\ f(I, B) & S\dfrac{\partial f}{\partial I} - (\gamma + b) & S\dfrac{\partial f}{\partial B} \\ 0 & \dfrac{\partial h}{\partial I} & \dfrac{\partial h}{\partial B} \end{pmatrix}.$$

The associated second compound matrix (see Appendix A) is given by

$$J^{[2]} = \begin{pmatrix} -(\gamma + 2b) - f(I, B) + S\dfrac{\partial f}{\partial I} & S\dfrac{\partial f}{\partial B} & S\dfrac{\partial f}{\partial B} \\ \dfrac{\partial h}{\partial I} & -b - f(I, B) + \dfrac{\partial h}{\partial B} & -S\dfrac{\partial f}{\partial I} \\ 0 & f(I, B) & S\dfrac{\partial f}{\partial I} + \dfrac{\partial h}{\partial B} - (\gamma + b) \end{pmatrix}.$$

We set the matrix function P by

$$P(S,I,B) = \operatorname{diag}\left\{1, \frac{I}{B}, \frac{I}{B}\right\}.$$

Then

$$P_F P^{-1} = \operatorname{diag}\left\{0, \frac{I'}{I} - \frac{B'}{B}, \frac{I'}{I} - \frac{B'}{B}\right\},$$

and

$$PJ^{[2]}P^{-1} = \begin{pmatrix} -(\gamma+2b) - f(I,B) + S\dfrac{\partial f}{\partial I} & \dfrac{SB}{I}\dfrac{\partial f}{\partial B} & \dfrac{SB}{I}\dfrac{\partial f}{\partial B} \\ \dfrac{I}{B}\dfrac{\partial h}{\partial I} & -b - f(I,B) + \dfrac{\partial h}{\partial B} & -S\dfrac{\partial f}{\partial I} \\ 0 & f(I,B) & S\dfrac{\partial f}{\partial I} + \dfrac{\partial h}{\partial B} - (\gamma+b) \end{pmatrix}.$$

The matrix $P_F P^{-1} + PJ^{[2]}P^{-1}$ defined in Equation (A2) can then be written in a block form:

$$Q = \begin{bmatrix} Q_{11} & Q_{12} \\ Q_{21} & Q_{22} \end{bmatrix},$$

with

$$Q_{11} = -(\gamma+2b) - f(I,B) + S\frac{\partial f}{\partial I}, \quad Q_{12} = \left[\frac{SB}{I}\frac{\partial f}{\partial B}, \frac{SB}{I}\frac{\partial f}{\partial B}\right],$$

$$Q_{21} = \begin{bmatrix} \dfrac{I}{B}\dfrac{\partial h}{\partial I} \\ 0 \end{bmatrix}, \quad Q_{22} = \begin{bmatrix} -b - f(I,B) + \dfrac{\partial h}{\partial B} + \dfrac{I'}{I} - \dfrac{B'}{B} & -S\dfrac{\partial f}{\partial I} \\ f(I,B) & -(\gamma+b) + S\dfrac{\partial f}{\partial I} + \dfrac{\partial h}{\partial B} + \dfrac{I'}{I} - \dfrac{B'}{B} \end{bmatrix}.$$

Now we define a norm in $\mathbb{R}^3$ as

$$|(u,v,w)| = \max\{|u|, |v| + |w|\}$$

for any vector $(u,v,w) \in \mathbb{R}^3$. Let m denote the Lozinskiĭ measure with respect to this norm. We can then obtain

$$m(Q) \le \sup\{g_1, g_2\}, \tag{12}$$

with

$$g_1 = m_1(Q_{11}) + |Q_{12}|,$$
$$g_2 = |Q_{21}| + m_1(Q_{22}),$$

where $|Q_{12}|$ and $|Q_{21}|$ are matrix norms induced by the L_1 vector norm, and m_1 denotes the Lozinskiĭ measure with respect to the L_1 norm. Specifically,

$$m_1(Q_{22}) = \frac{I'}{I} - \frac{B'}{B} - b + \frac{\partial h}{\partial B} + \sup\left\{2S\frac{\partial f}{\partial I} - \gamma, 0\right\}$$

and

$$g_2 = \frac{I}{B}\frac{\partial h}{\partial I} + \frac{I'}{I} - \frac{B'}{B} - b + \frac{\partial h}{\partial B} + \sup\left\{2S\frac{\partial f}{\partial I} - \gamma, 0\right\}.$$

Note that Equation (3) provides

$$\frac{B'}{B} = \frac{1}{B}h(I,B).$$

Also, based on the concavity of $h(I,B)$ (assumption **d**), it is easy to observe that

$$I\frac{\partial h}{\partial I}(I,B) + B\frac{\partial h}{\partial B}(I,B) \le h(I,B)$$

at any point (I,B). We thus obtain

$$\begin{aligned} g_2 &= \frac{1}{B}\left[I\frac{\partial h}{\partial I} + B\frac{\partial h}{\partial B} - h(I,B)\right] + \frac{I'}{I} - b + \sup\left\{2S\frac{\partial f}{\partial I} - \gamma, 0\right\} \\ &\le \frac{I'}{I} - b + \sup\left\{2S\frac{\partial f}{\partial I} - \gamma, 0\right\} \\ &\le \frac{I'}{I} - b, \end{aligned}$$

provided that

$$\max_{(S,I,B)\in\Delta}\left[2S\frac{\partial f}{\partial I}(I,B)\right] \le \gamma. \tag{13}$$

In particular, the condition (13) will be satisfied if

$$2N\max\frac{\partial f}{\partial I}(I,B) \le \gamma.$$

Meanwhile,

$$g_1 = -(\gamma + 2b) - f(I,B) + S\frac{\partial f}{\partial I} + \frac{SB}{I}\frac{\partial f}{\partial B}.$$

Based on Equation (2) and the concavity of $f(I,B)$, we have

$$\frac{I'}{I} = \frac{S}{I}f(I,B) - (\gamma + b)$$

and

$$I\frac{\partial f}{\partial I}(I,B) + B\frac{\partial f}{\partial B}(I,B) \le f(I,B).$$

We then obtain

$$\begin{aligned} g_1 &= \frac{I'}{I} - \frac{S}{I}f(I,B) - b - f(I,B) + S\frac{\partial f}{\partial I} + \frac{SB}{I}\frac{\partial f}{\partial B} \\ &= \frac{I'}{I} - b - f(I,B) + \frac{S}{I}\left[I\frac{\partial f}{\partial I} + B\frac{\partial f}{\partial B} - f(I,B)\right] \\ &\le \frac{I'}{I} - b. \end{aligned}$$

Therefore,

$$m(Q) \le \frac{I'}{I} - b. \tag{14}$$

Since $0 \le I(t) \le N$ and $\ln I(t) \le \ln N$, there exists $T > 0$ such that when $t > T$, $(1/t)[\ln I(t) - \ln I(0)] < b/2$; consequently,

$$\frac{1}{t}\int_0^t m(Q)\,\mathrm{d}t \le \frac{1}{t}\int_0^t\left(\frac{I'}{I} - b\right)\mathrm{d}t = \frac{\ln I(t) - \ln I(0)}{t} - b < -\frac{b}{2}, \tag{15}$$

which implies $\bar{q_2} \le -b/2 < 0$.

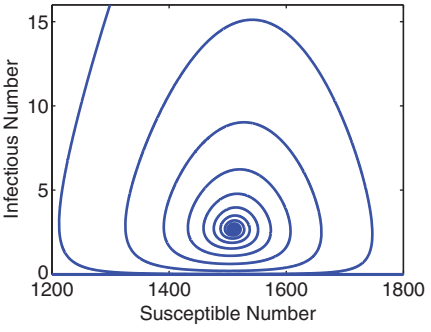

Figure 1. A phase portrait of S *vs* I for the cholera model (16)–(19). The total population is $N = 10,000$, and the initial condition is $I(0) = 1000$, $S(0) = 9000$ and $R(0) = B(0) = 0$. The curve converges to the endemic equilibrium at $S^* \approx 1510$, $I^* \approx 2.68$. Similar pattern is observed for various different initial conditions.

Hence, we have established the following theorem:

THEOREM 3.2 *When* $R_0 > 1$, *the unique endemic equilibrium of the three-dimensional system* (1)–(3) *is globally asymptotically stable in* Δ *under the assumptions* (**a**)–(**d**) *and* (13).

Remark 3.3 Theorem 3.2 establishes the global endemic stability for the unified three-dimensional cholera model. In particular, the result can be directly applied to several existing cholera models in the literature, such as those in [5,34,44].

To quantify the analysis, we consider the cholera model proposed by Mukandavire *et al.* [34]:

$$\frac{dS}{dt} = bN - \beta_e S\frac{B}{\kappa + B} - \beta_h SI - bS, \tag{16}$$

$$\frac{dI}{dt} = \beta_e S\frac{B}{\kappa + B} + \beta_h SI - (\gamma + b)I, \tag{17}$$

$$\frac{dB}{dt} = \xi I - \delta B, \tag{18}$$

$$\frac{dR}{dt} = \gamma I - bR. \tag{19}$$

Clearly, this is a special case of the general model (1)–(4). Figure 1 shows a typical phase portrait of S *vs* I for this model, based on numerical simulation. The parameter values are taken from [34] with $R_0 \approx 6.62$. The total population is normalized as $N = 10,000$, and the initial infection is set as $I(0) = 1000$. We observe a stable spiral and the solution curve eventually converges to the endemic equilibrium at $S^* \approx 1510$, $I^* \approx 2.68$. We have also tested many different initial conditions including $I(0) = 1, 10, 100$, and 2000, and all these solution curves (not shown here) approach the endemic equilibrium over time, with very similar pattern to that in Figure 1.

4. Four-dimensional system

We now consider the model (1)–(3) in the case when B is a vector; i.e. there are heterogeneous and multiple states of infectivity for the pathogen outside the human hosts. The representation of pathogen dynamics in multiple states can possibly provide a deeper insight into the pathogen ecology and the complex interaction between the human hosts and the environment, and reflect

better the nature of heterogeneity in disease transmission. Without loss of generality, we assume $B = [B_1, B_2]$, where B_1 and B_2 represent two different infectious states of the bacterial concentrations. A similar formulation of B was used in [13], where the HI and LI states of the vibrios were modelled. Multiple states of cholera bacterial concentrations were also studied in [39].

We consider the following four-dimensional system corresponding to the model (1)–(3):

$$\frac{\mathrm{d}S}{\mathrm{d}t} = bN - Sf(I, B_1, B_2) - bS, \tag{20}$$

$$\frac{\mathrm{d}I}{\mathrm{d}t} = Sf(I, B_1, B_2) - (\gamma + b)I, \tag{21}$$

$$\frac{\mathrm{d}B_1}{\mathrm{d}t} = h_1(I, B_1, B_2), \tag{22}$$

$$\frac{\mathrm{d}B_2}{\mathrm{d}t} = h_2(I, B_1, B_2). \tag{23}$$

The functions f and $h = [h_1, h_2]^{\mathrm{T}}$ have to satisfy conditions (**a**)–(**d**), noting that $\partial f/\partial B$ and $\partial h/\partial I$ are vectors and that $-\partial h/\partial B$ is an M-matrix (see Remark 2.1). It is easy to observe that the mass action bilinear incidence $f(I, B_1, B_2) = \beta I + \beta_1 B_1 + \beta_2 B_2$ and the saturated incidence $f(B1, B_2) = \beta_1 B_1/(K_1 + B_1) + \beta_2 B_2/(K_2 + B_2)$ satisfy these assumptions. Meanwhile, we note that conditions (**c**) and (**d**) imply

$$h(I, B) \le h(N, B) \le h(N, 0) + \frac{\partial h}{\partial B}(N, 0)B \tag{24}$$

for all $I, B \ge 0$.

Let

$$B_0 = -\left(\frac{\partial h}{\partial B}(N, 0)\right)^{-1} h(N, 0) > 0, \tag{25}$$

due to fact that $-(\partial h/\partial B)(N, 0)$ is an M-matrix. From Equations (22), (23) and the inequality (24), we see that if $(B_1(0), B_2(0)) \le B_0^{\mathrm{T}}$, then $(B_1(t), B_2(t)) \le B_0^{\mathrm{T}}$ for all $t \ge 0$. Hence, the feasible region

$$\Gamma = \{(S, I, B_1, B_2) | S \ge 0, I \ge 0, S + I \le N, 0 \le (B_1, B_2) \le B_0^{\mathrm{T}}\} \tag{26}$$

is invariant under the flow of (20)–(23). Moreover, we have

PROPOSITION 4.1 *For any $\varepsilon > 0$ and any initial value $B_1(0), B_2(0) > 0$, there is a constant $T = T(\varepsilon, B_1(0), B_2(0)) > 0$ such that*

$$(B_1(t), B_2(t)) \le B_0^{\mathrm{T}} + \varepsilon \tag{27}$$

for all $t > T$.

Similar to Proposition 3.1, the instability of the DFE $(N, 0, 0, 0)$, which is on the boundary of the domain Γ, implies uniform persistence [11]. Based on Theorem 2.2, we thus obtain

PROPOSITION 4.2 *When $R_0 > 1$, the system* (20)–(23) *is uniformly persistent.*

We now prove the main result in this section, i.e. the global stability of the endemic equilibrium, using the geometric approach based on the third compound matrix (see Appendix B). To simplify

our notations, we will adopt the abbreviations

$$f_0' = \frac{\partial f}{\partial I}, \quad f_1' = \frac{\partial f}{\partial B_1}, \quad f_2' = \frac{\partial f}{\partial B_2}, \quad h_{i0}' = \frac{\partial h_i}{\partial I}, \quad h_{ij}' = \frac{\partial h_i}{\partial B_j}, \quad i,j = 1,2.$$

We will also need the following inequalities, which can be easily derived based on the assumptions (**a**)–(**d**):

$$If_0' + B_1 f_1' + B_2 f_2' \le f, \tag{28}$$

$$Ih_{10}' + B_1 h_{11}' + B_2 h_{12}' \le h_1, \tag{29}$$

$$Ih_{20}' + B_1 h_{21}' + B_2 h_{22}' \le h_2, \tag{30}$$

for all $I, B \ge 0$. In particular, we have

$$If_0' \le f, \quad B_1 f_1' \le f, \quad B_2 f_2' \le f. \tag{31}$$

THEOREM 4.3 *If* $R_0 > 1$ *and*

$$f_0' \le \frac{b}{N}, \tag{32}$$

then the unique endemic equilibrium of the four-dimensional system (20)–(23) *is globally asymptotically stable in* Γ *provided that the conditions* (**a**)–(**d**) *hold.*

Proof The Jacobian matrix of the system (20)–(23) is given by

$$J = \begin{pmatrix} -b-f & -Sf_0' & -Sf_1' & -Sf_2' \\ f & Sf_0' - b - \gamma & Sf_1' & Sf_2' \\ 0 & h_{10}' & h_{11}' & h_{12}' \\ 0 & h_{20}' & h_{21}' & h_{22}' \end{pmatrix}.$$

The third additive compound matrix of J is

$$J^{[3]} = \begin{pmatrix} Sf_0' + h_{11}' - 2b - \gamma - f & h_{12}' & -Sf_2' & -Sf_2' \\ h_{21}' & Sf_0' + h_{22}' - 2b - \gamma - f & Sf_1' & Sf_1' \\ -h_{20}' & h_{10}' & h_{11}' + h_{22}' - b - f & -Sf_0' \\ 0 & 0 & f & h_{11}' + h_{22}' + Sf_0' - b - \gamma \end{pmatrix}$$

and the associated linear compound system is

$$X' = (Sf_0' + h_{11}' - 2b - \gamma - f)X + h_{12}'Y - Sf_2'W - Sf_2'Z, \tag{33}$$

$$Y' = h_{21}'X + (Sf_0' + h_{22}' - 2b - \gamma - f)Y + Sf_1'W + Sf_1'Z, \tag{34}$$

$$W' = -h_{20}'X + h_{10}'Y + (h_{11}' + h_{22}' - b - f)W - Sf_0'Z, \tag{35}$$

$$Z' = fW + (h_{11}' + h_{22}' + Sf_0' - b - \gamma)Z. \tag{36}$$

As in [26,27] (also see Appendix B), we need to show the uniform global stability of the linear compound system (33)–(36). To this end, we choose an associated Lyapunov function

$$V(t, X, Y, W, Z) = \max\{V_1, V_2, V_3\},$$

where

$$V_1 = B_2|X|, \quad V_2 = B_1|Y|, \quad V_3 = \begin{cases} I|W+Z|, & WZ \geq 0, \\ \max\{I|W|, I|Z|\}, & WZ < 0. \end{cases}$$

It is easy to see that the following estimate holds:

$$I|W+Z| \leq V_3, \quad (W,Z) \in \mathbb{R}^2. \tag{37}$$

Based on Propositions 4.1 and 4.2, we see that there exist positive constants C_1 and C_2 such that

$$C_1(|X|+|Y|+|W|+|Z|) \leq V \leq C_2(|X|+|Y|+|W|+|Z|). \tag{38}$$

Meanwhile, by Equation (32) and the uniform persistence of the system, we can choose a (small) constant $k > 0$ such that

$$f, b, \gamma \geq k. \tag{39}$$

Next, we calculate the total derivative of V along the trajectory of the compound system (33)–(36). We will separate the discussion for the several cases below.

Case I: $V = V_1$, then $V_2, V_3 \leq V_1$ and

$$\begin{aligned} D_+V &\leq B_2'|X| + B_2 D_+|X| \\ &\leq B_2'|X| + (h_{11}' + Sf_0' - 2b - \gamma - f)B_2|X| + h_{12}'B_2|Y| + SB_2f_2'(|W+Z|) \\ &\leq \left[\frac{B_2'}{B_2} + \frac{B_1h_{11}' + B_2h_{12}'}{B_1} + Sf_0' - 2b - \gamma - f + \frac{SB_2f_2'}{I}\right]B_2|X| \\ &\leq \left[\frac{B_2'}{B_2} + \frac{h_1}{B_1} + Sf_0' - 2b - \gamma - f + \frac{Sf}{I}\right]B_2|X| \\ &= \left[\frac{B_2'}{B_2} + \frac{B_1'}{B_1} + \frac{I'}{I} + Sf_0' - b - f\right]V \\ &\leq \left[\frac{B_2'}{B_2} + \frac{B_1'}{B_1} + \frac{I'}{I} - k\right]V, \end{aligned} \tag{40}$$

since $I|W+Z| \leq V_3$ by Equation (37), $(B_1h_{11}' + B_2h_{12}')/B_1 \leq (Ih_{10}' + B_1h_{11}' + B_2h_{12}')/B_1 \leq h_1/B_1 = B_1'/B_1$ by Equation (29), $SB_2f_2'/I \leq Sf/I = b + \gamma + I'/I$ by (31), $Sf_0' - b \leq 0$ by Equation (32), and $f \geq k$ by Equation (39). Here and in what follows D_+ denotes the right-hand (total) derivative with respect to t.

Case II: $V = V_2$, then $V_1, V_3 \leq V_2$. In a way similar to Case I, we can obtain the estimates

$$\begin{aligned} D_+V &\leq B_1'|Y| + B_1 D_+|Y| \\ &\leq B_1'|Y| + h_{21}'B_1|X| + (h_{22}' + Sf_0' - 2b - \gamma - f)B_1|Y| + SB_1f_1'(|W+Z|) \\ &\leq \left[\frac{B_1'}{B_1} + \frac{B_1h_{21}' + B_2h_{22}'}{B_2} + Sf_0' - b - f + \frac{SB_1f_1'}{I}\right]B_1|Y| \\ &\leq \left[\frac{B_1'}{B_1} + \frac{h_2}{B_2} + Sf_0' - 2b - \gamma - f + \frac{Sf}{I}\right]V \\ &= \left[\frac{B_2'}{B_2} + \frac{B_1'}{B_1} + \frac{I'}{I} + Sf_0' - b - f)\right]V \\ &\leq \left[\frac{B_2'}{B_2} + \frac{B_1'}{B_1} + \frac{I'}{I} - k\right]V, \end{aligned} \tag{41}$$

where $(B_1h'_{21} + B_2h'_{22})/B_2 \le (Ih'_{20} + B_1h'_{21} + B_2h'_{22})/B_2 \le h_2/B_2 = B'_2/B_2$ by Equation (30), and $SB_1f'_1/I \le Sf/I = b + \gamma + I'/I$ by Equation (31).

Case III-a: $V = I|W + Z|$, then $V_1, V_2 \le I|W + Z| = V_3$ and

$$\begin{aligned} D_+V &\le I'(|W + Z|) + ID_+(|W + Z|) \\ &\le \left(\frac{I'}{I} + h'_{11} + h'_{22} - b\right) V_3 + h'_{20}I|X| + h'_{10}I|Y| - \gamma I|Z| \\ &\le \left(\frac{I'}{I} + h'_{11} + h'_{22} - b\right) V_3 + h'_{20}I|X| + h'_{10}I|Y| \\ &\le \left(\frac{I'}{I} + h'_{11} + h'_{22}\right) V_3 + h'_{20}I|X| + h'_{10}I|Y| - kV_3 \\ &\le \left[\frac{I'}{I} + \frac{Ih'_{10} + B_1h'_{11}}{B_1} + \frac{Ih'_{20} + B_2h'_{22}}{B_2} - k\right] V_3 \\ &\le \left[\frac{I'}{I} + \frac{h_1}{B_1} + \frac{h_2}{B_2} - k\right] V \\ &= \left[\frac{I'}{I} + \frac{B'_1}{B_1} + \frac{B'_2}{B_2} - k\right] V, \end{aligned} \tag{42}$$

since $(Ih'_{10} + B_1h'_{11})/B_1 \le h_1/B_1$, $(Ih'_{20} + B_2h'_{22})/B_2 \le h_2/B_2$ by Equations (29) and (30), and $k \le b$ by Equation (39).

Case III-b: $V = I|W|$, then $WZ < 0$, $V_1, V_2, I|Z| \le I|W| = V_3$, and

$$\begin{aligned} D_+V &\le I'|W| + ID_+|W| \\ &\le \left(\frac{I'}{I} + h'_{11} + h'_{22} - b - f\right) V_3 + h'_{20}I|X| + h'_{10}I|Y| + Sf'_0I|Z| \\ &\le \left(\frac{I'}{I} + h'_{11} + h'_{22} - b - f + Sf'_0\right) V_3 + h'_{20}I|X| + h'_{10}I|Y| \\ &\le \left[\frac{I'}{I} + \frac{Ih'_{10} + B_1h'_{11}}{B_1} + \frac{Ih'_{20} + B_2h'_{22}}{B_2} - k\right] V_3 \\ &\le \left[\frac{I'}{I} + \frac{h_1}{B_1} + \frac{h_2}{B_2} - k\right] V \\ &= \left[\frac{I'}{I} + \frac{B'_1}{B_1} + \frac{B'_2}{B_2} - k\right] V. \end{aligned} \tag{43}$$

Case III-c: $V = I|Z|$, then $WZ < 0$, $V_1, V_2, I|W| \le I|Z| = V_3$. Using similar estimates and the condition $\gamma \ge k$, we obtain

$$\begin{aligned} D_+V &\le I'|Z| + ID_+|Z| \\ &\le \left(\frac{I'}{I} + h'_{11} + h'_{22} + Sf'_0 - b - \gamma\right) V_3 - fI|W| \\ &\le \left(\frac{I'}{I} + h'_{11} + h'_{22} - b - f + Sf'_0\right) V_3 \\ &\le \left[\frac{I'}{I} + \frac{Ih'_{10} + B_1h'_{11}}{B_1} + \frac{Ih'_{20} + B_2h'_{22}}{B_2} - k\right] V_3 \end{aligned}$$

$$\leq \left[\frac{I'}{I} + \frac{h_1}{B_1} + \frac{h_2}{B_2} - k\right] V$$
$$= \left[\frac{I'}{I} + \frac{B_1'}{B_1} + \frac{B_2'}{B_2} - k\right] V. \tag{44}$$

Now, let $K(t) = \ln(IB_1B_2)$. Then it follows from (40) to (44) that the following estimate holds:

$$D_+V \leq [(K(t))' - k]V. \tag{45}$$

In view of Propositions 4.1 and 4.2, there is a constant $C > 0$ such that

$$C \geq K(t) \geq C^{-1}, \tag{46}$$

for sufficiently large t. Therefore, we conclude from Equations (38), (45), (46) and Theorem A.2 (see Appendix B) that the endemic equilibrium of the system (20)–(23) is globally asymptotically stable. Indeed, there exists $s > 0$ such that for all $t \geq s$,

$$V(t) \leq \frac{K(t)}{K(s)} V(s)\, \mathrm{e}^{-k(t-s)} \leq C^2 V(s)\, \mathrm{e}^{-k(t-s)},$$

implying the uniform global stability of the associated linear compound system. The proof is thus complete. ■

Remark 4.4 Theorem 4.3 establishes the global endemic stability for a general four-dimensional cholera model. As a special case, the result can be directly applied to the cholera model in [13]. We note, however, that the assumption in (32) is a sufficient condition for the global stability and it might restrict the applicability of the result.

Remark 4.5 The analysis presented here can be easily extended to the case with variable host population, where we incorporate immigration and disease-related mortality into the model (20)–(23). Thus, Equations (20) and (21) will be replaced by

$$\frac{\mathrm{d}S}{\mathrm{d}t} = N_0 - Sf(I, B_1, B_2) - bS, \tag{47}$$
$$\frac{\mathrm{d}I}{\mathrm{d}t} = Sf(I, B_1, B_2) - (\gamma + b + b_0)I, \tag{48}$$

where N_0 is the immigration rate and b_0 is the disease caused death rate (for cholera, this is usually lower than 1% [48]). In this case, the total human population $N = S + I + R$ is not a constant but satisfies

$$\frac{\mathrm{d}N}{\mathrm{d}t} = N_0 - bN - b_0 I \leq N_0 - bN.$$

If we define

$$\tilde{B}_0 = -\left(\frac{\partial h}{\partial B}\right)^{-1} h\left(\frac{N_0}{b}, 0\right),$$

then the feasible domain becomes

$$\tilde{\Gamma} = \left\{(S, I, B_1, B_2) | S \geq 0, I \geq 0, S + I \leq \frac{N_0}{b},\ 0 \leq (B_1, B_2) \leq \tilde{B}_0^{\mathrm{T}}\right\}.$$

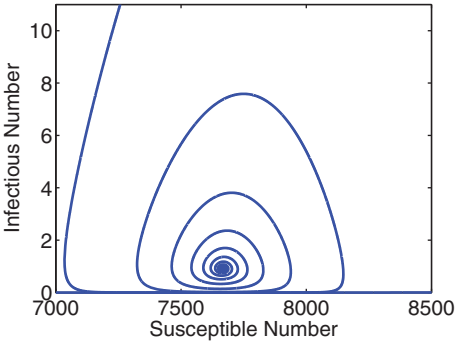

Figure 2. A phase portrait of S *vs* I for the cholera model (49)–(53). The total population is $N = 10,000$, and the initial condition is $I(0) = 1000, S(0) = 9000$, and $R(0) = B_H(0) = B_H(0) = 0$. The curve converges to the endemic equilibrium at $S^* \approx 7666$ and $I^* \approx 0.92$. Similar pattern is observed for various different initial conditions.

Correspondingly, the constraint on f_0' in Theorem 4.3 is replaced by

$$f_0' \leq \frac{b^2}{N_0}.$$

Then the same analysis as presented in this section can be applied to establish the global asymptotic stability of the endemic equilibrium for this variable population model.

Finally, we present an example to verify the analytical prediction in Theorem 4.3. We consider the cholera model of Hartley *et al.* [13]:

$$\frac{dS}{dt} = bN - \beta_L S\frac{B_L}{\kappa_L + B_L} - \beta_H S\frac{B_H}{\kappa_H + B_H} - bS, \tag{49}$$

$$\frac{dI}{dt} = \beta_L S\frac{B_L}{\kappa_L + B_L} + \beta_H S\frac{B_H}{\kappa_H + B_H} - (\gamma + b)I, \tag{50}$$

$$\frac{dB_H}{dt} = \xi I - \chi B_H, \tag{51}$$

$$\frac{dB_L}{dt} = \chi B_H - \delta_L B_L, \tag{52}$$

$$\frac{dR}{dt} = \gamma I - bR. \tag{53}$$

Using numerical simulation, we obtain a typical phase portrait of S *vs* I for this model, shown in Figure 2. The parameter values are taken from [13,30] with $R_0 \approx 1.31$. Again the total population is normalized as $N = 10,000$, and the initial infection is set as $I(0) = 1000$. The solution curve approaches the endemic equilibrium at $S^* \approx 7666, I^* \approx 0.92$ over time. It is also observed (though not shown here) that solutions with various different initial conditions converge to the same endemic equilibrium, a verification of its global asymptotical stability.

5. Conclusions

The present work aims to understand the global dynamics of cholera epidemiology in a general mathematical model which has a potential to incorporate different factors of the human host, the environment, and the pathogen ecology into a unified framework. Such an understanding is

important for the effective prevention and intervention strategies against cholera outbreak. The unified global stability results established in this paper can be applied to many published cholera models, including (but not limited to) those in [5,13,18,34,44,47].

Due to the incorporation of the environmental component and the coupling of multiple transmission pathways, the cholera model considered in this paper distinguishes itself from regular SIR and SEIR epidemiological models whose global dynamics have been extensively studied [15,16,22–24,27,29,32,49]. Using the geometric approach, we have carefully investigated both three-dimensional and four-dimensional systems under general settings. The analysis and results presented in this paper not only extend the application of the geometric approach, but also provide a framework for modelling and analysing other infectious diseases such as typhoid fever, amoebiasis, dracunculiasis, giardia, cryptosporidium, and campylobacter [31,44] which involve environmental components (e.g. water-borne pathogen).

Acknowledgements

J. Wang acknowledges partial support from the National Science Foundation (under Grant No. DMS-0813691) and the Simons Foundation (under Grant No. 208716). The authors thank the two anonymous referees for their helpful comments to improve this paper.

References

[1] A. Alam, R.C. LaRocque, J.B. Harris, C. Vanderspurt, E.T. Ryan, F. Qadri, and S.B. Calderwood, *Hyperinfectivity of human-passaged Vibrio cholerae can be modeled by growth in the infant mouse*, Infect. Immun. 73 (2005), pp. 6674–6679.
[2] A. Berman and R.J. Plemmons, *Nonnegative Matrices in the Mathematical Sciences*, SIAM, Philadelphia, 1994.
[3] B. Buonomo and D. Lacitignola, *On the use of the geometric approach to global stability for three dimensional ODE systems: A bilinear case*, J. Math. Anal. Appl. 348 (2008), pp. 255–266.
[4] G.J. Butler and P. Waltman, *Persistence in dynamical systems*, Proc. Amer. Math. Soc. 96 (1986), pp. 425–430.
[5] C.T. Codeço, *Endemic and epidemic dynamics of cholera: The role of the aquatic reservoir*, BMC Infect. Dis. 1(1) (2001).
[6] W.A. Coppel, *Stability and Asymptotical Behavior of Differential Equations*, Heath Mathematical Monographs, D. C. Heath, Boston, MA, 1965.
[7] G.W. Cross, *Three types of matrix stability*, Linear Algebra Appl. 20 (1978), pp. 253–263.
[8] P. van den Driessche and J. Watmough, *Reproduction numbers and sub-threshold endemic equilibria for compartmental models of disease transmission*, Math. Biosci. 180 (2002), pp. 29–48.
[9] M. Fan, M.Y. Li, and K. Wang, *Global stability of an SEIS epidemic model with recruitment and a varying total population size*, Math. Biosci. 170 (2001), pp. 199–208.
[10] S. Faruque, M. Islam, Q. Ahmad, A.S.G. Faruque, D. Sack, G. Nair, and J. Mekalanos, *Self-limiting nature of seasonal cholera epidemics: Role of host-mediated amplification of phage*, Proc. Nat. Acad. Sci. 102 (2005), pp. 6119–6124.
[11] H.I. Freedman, S. Ruan, and M. Tang, *Uniform persistence and flows near a closed positively invariant set*, J. Dyn. Differential Equations 6 (1994), pp. 583–600.
[12] K. Goh, S. Teo, S. Lam, and M. Ling, *Person-to-person transmission of cholera in a psychiatric hospital*, J. Inf. 20 (1990), pp. 193–200.
[13] D.M. Hartley, J.G. Morris, and D.L. Smith, *Hyperinfectivity: A critical element in the ability of V. cholerae to cause epidemics?* PLoS Med. 3 (2006), pp. 0063–0069.
[14] P. Hartman, *Ordinary Differential Equations*, John Wiley, New York, 1980.
[15] H.W. Hethcote, *Qualitative analysis of communicable disease models*, Math. Biosci. 28 (1976), pp. 335–356.
[16] H.W. Hethcote, *The mathematics of infectious diseases*, SIAM Rev. 42 (2000), pp. 599–653.
[17] M. Jensen, S.M. Faruque, J.J. Mekalanos, and B. Levin, *Modeling the role of bacteriophage in the control of cholera outbreaks*, Proc. Nat. Acad. Sci. 103 (2006), pp. 4652–4657.
[18] R.I. Joh, H. Wang, H. Weiss, and J.S. Weitz, *Dynamics of indirectly transmitted infectious diseases with immunological threshold*, Bull. Math. Biol. 71 (2009), pp. 845–862.
[19] H.K. Khalil, *Nonlinear Systems*, Prentice-Hall, Englewood Cliffs, NJ, 1996.
[20] A.A. King, E.L. Lonides, M. Pascual, and M.J. Bouma, *Inapparent infections and cholera dynamics*, Nature 454 (2008), pp. 877–881.
[21] A. Lajmanovich and J. Yorke, *A deterministic model for gonorrhea in a nonhomogeneous population*, Math. Biosci. 28 (1976), pp. 221–236.
[22] G. Li and Z. Jin, *Global stability of an SEI epidemic model with general contact rate*, Chaos, Solitons Fractals 23 (2005), pp. 997–1004.

[23] M.Y. Li, J.R. Graef, L. Wang, and J. Karsai, *Global dynamics of a SEIR model with varying total population size*, Math. Biosci. 160 (1999), pp. 191–213.
[24] M.Y. Li and J.S. Muldowney, *Global stability for the SEIR model in epidemiology*, Math. Biosci. 125 (1995), pp. 155–164.
[25] M.Y. Li and J.S. Muldowney, *A geometirc approach to global-stability problems*, SIAM J. Math. Anal. 27 (1996), pp. 1070–1083.
[26] M.Y. Li and J.S. Muldowney, *Dynamics of differential equations on invariant manifolds*, J. Differential Equations 168 (2000), pp. 295–320.
[27] M.Y. Li, J.S. Muldowney, and P.V.D. Driessche, *Global stability of SEIRS models in epidemiology*, Can. Appl. Math. Q. 7 (1999), pp. 409–425.
[28] M.Y. Li, H.L. Smith, and L. Wang, *Global dynamics of an SEIR epidemic model with vertical transmission*, SIAM J. Math. Anal. 62 (2001), pp. 58–69.
[29] M.Y. Li and L. Wang, *Global stability in some SEIR epidemic models*, IMA Volumes in Mathematics and Its Application Vol. 126, Springer-Verlag, Berlin, 2002, pp. 295–311.
[30] S. Liao and J. Wang, *Stability analysis and application of a mathematical cholera model*, Math. Biosci. Eng. 8 (2011), pp. 733–752.
[31] S. Ma and Y. Xia (Eds.), *Mathematical Understanding of Infectious Disease Dynamics*, Lecture Notes Series Vol. 16, Institute for Mathematical Sciences, National University of Singapore, Singapore, 2008.
[32] J. Mena-Lorca and H.W. Hethcote, *Dynamic models of infectious diseases as regulator of population sizes*, J. Math. Biol. 30 (1992), pp. 693–716.
[33] D.S. Merrell, S.M. Butler, F. Qadri, N.A. Dolganov, A. Alam, M.B. Cohen, S.B. Calderwood, G.K. Schoolnik, and A. Camilli, *Host-induced epidemic spread of the cholera bacterium*, Nature 417 (2002), pp. 642–645.
[34] Z. Mukandavire, S. Liao, J. Wang, H. Gaff, D.L. Smith, and J.G. Morris, *Estimating the reproductive numbers for the 2008–2009 cholera outbreaks in Zimbabwe*, Proc. Nat. Acad. Sci. 108 (2011), pp. 8767–8772.
[35] J.S. Muldowney, *Compound matrices and ordinary differential equations*, Rocky Mountain J. Math. 20 (1990), pp. 857–872.
[36] E.J. Nelson, J.B. Harris, J.G. Morris, S.B. Calderwood and A. Camilli, *Cholera transmission: The host, pathogen and bacteriophage dynamics*, Nat. Rev.: Microbiol. 7 (2009), pp. 693–702.
[37] M. Pascual, X. Rodo, S.P. Ellner, R. Colwell, and M.J. Bouma, *Cholera dynamics and El Nino-Southern oscillation*, Science 289 (2000), pp. 1766–1769.
[38] M. Pascual, M. Bouma, and A. Dobson, *Cholera and climate: Revisiting the quantiative evidence*, Microbes Infections 4 (2002), pp. 237–245.
[39] Z. Shuai and P. van den Driessche, *Global dynamics of cholera models with differential infectivity*, Math. Biosci. 234 (2011), pp. 118–126.
[40] H.L. Smith, *Monotone Dynamical Systems: An Introduction to the Theory of Competitive and Cooperative Systems*, American Mathematical Society, Providence, RI, 1995.
[41] H.L. Smith and H.R. Zhu, *Stable periodic orbits for a class of three dimensional competitive systems*, J. Differential Equations 110 (1994), pp. 143–156.
[42] R.A. Smith, *Orbital stability for ordinary differential equations*, J. Differential Equations 69 (1987), pp. 265–287.
[43] J.P. Tian and J. Wang, *Global stability for cholera epidemic models*, Math. Biosci. 232 (2011), pp. 31–41.
[44] J.H. Tien and D.J.D. Earn, *Multiple transmission pathways and disease dynamics in a waterborne pathogen model*, Bull. Math. Biol. 72 (2010), pp. 1502–1533.
[45] V. Tudor and I. Strati, *Smallpox, Cholera*, Abacus Press, Tunbridge Wells, 1977.
[46] E. Vynnycky, A. Trindall, and P. Mangtani, *Estimates of the reproduction numbers of Spanish influenza using morbidity data*, Int. J. Epidemiol. 36 (2007), pp. 881–889.
[47] J. Wang and S. Liao, *A generalized cholera model and epidemic/endemic analysis*, J. Biol. Dyn. 6 (2012), pp. 568–589.
[48] World Health Organization, Available at web page: www.who.org.
[49] J. Zhang and Z. Ma, *Global dynamics of an SEIR epidemic model with saturating contact rate*, Math. Biosci. 185 (2003), pp. 15–32.

Appendix A

We briefly describe below the geometric approach based on the second additive compound matrix, developed by Li and Muldowney [9,25,28].

For a 3×3 matrix $A = [a_{ij}]$, the second additive compound matrix is defined as

$$A^{[2]} = \begin{pmatrix} a_{11} + a_{22} & a_{23} & -a_{13} \\ a_{32} & a_{11} + a_{33} & a_{12} \\ -a_{31} & a_{21} & a_{22} + a_{33} \end{pmatrix}.$$

We refer to [35] for a survey of general compound matrices.

Now consider the dynamical system

$$\frac{\mathrm{d}X}{\mathrm{d}t} = F(X), \tag{A1}$$

where $F : D \mapsto \mathbb{R}^n$ is a C^1 function and where $D \subset \mathbb{R}^n$ is a simply connected open set. Let $X(t, X_0)$ denote the solution of Equation (A1) with the initial condition $X(0) = X_0$. We assume:

(H1) There exists a compact absorbing set $K \subset D$;
(H2) The system (A1) has a unique equilibrium point X^* in D.

It is shown in [9,25,28] that X^* is globally asymptotically stable if (A1) satisfies (H1)(H2) and a Bendixson criterion that is robust under C^1 local perturbations of F at all non-equilibrium non-wandering points. This criterion is obtained as follows.

Let $X \mapsto P(X)$ be a $\binom{n}{2} \times \binom{n}{2}$ matrix-valued C^1 function in D. Set

$$Q = P_F P^{-1} + P J^{[2]} P^{-1}, \tag{A2}$$

where P_F is the derivative of P (entry-wise) along the direction of F and $J^{[2]}$ is the second compound matrix of the Jacobian $J(X) = DF(X)$. Let $m(Q)$ be the Lozinskiĭ measure of Q with respect to a matrix norm [6], i.e.

$$m(Q) = \lim_{h \to 0^+} \frac{|I + hQ| - 1}{h}. \tag{A3}$$

Define a quantity $\bar{q}_2$ as

$$\bar{q}_2 = \limsup_{t \to \infty} \sup_{X_0 \in K} \frac{1}{t} \int_0^t m(Q(X(s, X_0)))\, \mathrm{d}s. \tag{A4}$$

Then the Bendixson criterion is given by

$$\bar{q}_2 < 0. \tag{A5}$$

In summary, we have the following theorem:

THEOREM A.1 *Assume that D is simply connected and the assumptions* (H1) *and* (H2) *hold. Then the unique equilibrium* X^* *of (A1) is globally asymptotically stable in D if* $\bar{q}_2 < 0$.

Appendix B

In what follows, we outline the geometric approach based on the third additive compound matrix [26,27].

The third additive compound matrix for a 4×4 matrix $A = [a_{ij}]$ is defined as

$$A^{[3]} = \begin{pmatrix} a_{11} + a_{22} + a_{33} & a_{34} & -a_{24} & a_{14} \\ a_{43} & a_{11} + a_{22} + a_{44} & a_{23} & -a_{13} \\ -a_{42} & a_{32} & a_{11} + a_{33} + a_{44} & a_{12} \\ a_{41} & -a_{31} & a_{21} & a_{22} + a_{33} + a_{44} \end{pmatrix}.$$

For a solution $X(t, X_0)$ of any initial value problem of the dynamic system (A1), the linearized system is

$$Y' = J(X(t, X_0))Y,$$

and the associated third compound system is

$$Z' = J^{[3]}(X(t, X_0))Z, \tag{A6}$$

where $J^{[3]}$ is the third compound matrix of the Jacobian J for equation (A1).

THEOREM A.2 *Assume that* (H1) *and* (H2) *hold and there are a Lyapunov function* $V(X, Z)$, *a function* $K(t)$, *and positive constants c, k, and C such that*

(i) $c|Z| \le V(X, Z) \le C|Z|, \quad c \le K(t) \le C,$
(ii) $V' \le (K'(t) - k)V,$

where the total derivative V' *is taken along the direction of Equation* (A6), *then the interior equilibrium* X^* *of Equation* (A1) *is globally asymptotically stable.*

Proof If $K(t) = \text{Const.}$, this is the Corollary 3.2 in [27]. For a general differentiable function $K(t)$, the conclusion follows from the Corollary 3.2 in [27], since the modified Lyapunov function $\tilde{V} = V(X, Z)/K(t)$ satisfies all the conditions. ■